



Transport of nitrogen gas in glassy maltodextrins

Giovanni M. Falco^{a,b,*}, Albert T. Poortinga^a, S. Martinus Oversteegen^{a,1}

^a FrieslandCampina Research, Harderwijkerstraat 6, 7418 BA Deventer, The Netherlands

^b Institut für Theoretische Physik, Universität zu Köln, Zùlpicher Strasse 77, D-50937 Köln, Germany

ARTICLE INFO

Article history:

Received 4 June 2012

Received in revised form

25 September 2012

Accepted 18 October 2012

Available online 14 November 2012

Keywords:

Diffusion

Sorption

Glassy polymers

Carbohydrates

Free-volume

ABSTRACT

Glassy maltodextrins are amorphous carbohydrates characterized by very high barrier properties for low molecular weight gases. Although they are commonly used for the encapsulation of active ingredients in food and pharmaceuticals, the microscopic description of the processes which limit the diffusion of molecules inside the polymeric glassy matrix is still not fully understood. In this paper, we study sorption and diffusion of nitrogen molecules in glassy maltodextrins at negligible water content. The solution–diffusion model for the transport of small molecules is combined with recent positron annihilation lifetime spectroscopy data on the microscopic structure of the matrices. We find that both sorption and diffusion are strongly suppressed by the reduced size of the hole volumes and by the enhanced rigidity of the glassy carbohydrates matrices. Values of the diffusion coefficient of nitrogen gas in glassy maltodextrin calculated using the transition state theory were found to correspond well with experimentally obtained values. Also, our calculations can explain the recently observed remarkably high stability of pressurized nitrogen encapsulated in maltodextrin.

© 2012 Elsevier B.V. All rights reserved.

1. Introduction

The knowledge of the diffusion constant of small penetrant molecules in polymers is of crucial importance for many technological applications, such as design of barrier materials and gas-separating membranes. Stimulated by these applications, the diffusion of small penetrants in synthetic polymer membranes in both rubbery and glassy state has been extensively investigated [1]. Much less is known about the molecular processes involved in sorption and diffusion of small penetrants in dense matrices of carbohydrates polymers.

The good barrier properties of amorphous glassy carbohydrates have been recognized since long [2–5]. For this reason and thanks to their ability to form matrices of adjustable morphology, carbohydrates are often used for the encapsulation of oxygen-sensitive active ingredients and of volatile flavors [3,6,7]. The good barrier properties of glassy carbohydrates are also utilized to maintain the activity during storage of dried biological materials such as cells and vaccines [8,9]. Despite this practical importance, a theoretical description that explains the barrier properties of glassy carbohydrates is still lacking and attempts to predict the diffusion constant of low molecular solutes in glassy

carbohydrates have at best been semi-empirical [4,10]. For example, the Stokes–Einstein equation has been used to calculate the diffusion constant from the measured viscosity of the matrix, but this led to a gross underestimation of the diffusion constant [4,10]. It has been recognized that a better understanding of transport phenomena in glassy carbohydrates is needed to further optimize the barrier properties of e.g. food materials [3]. As an example of the exceptional barrier properties of glassy carbohydrates it was recently discovered that nitrogen gas under pressure can be stored in maltodextrin powders for more than a year [11–13]. Looking at the permeability coefficients of common synthetic polymers this is a surprisingly long time, indicating that glassy carbohydrates exhibit exceptionally low permeabilities. This stimulated us to try to calculate the permeability coefficient of gasses in glassy carbohydrates from first principles.

In this paper, we investigate the mechanisms inside polymeric, specifically maltodextrin, glassy matrices at negligible water content, that may limit the diffusion of the incorporated gas molecules. The paper is organized as follows. In Section 2 we introduce the physics of the solution–diffusion model [1] for the transport of gases in densely packed glassy carbohydrate matrices. In Section 3 we analyze the diffusion constant of nitrogen in glassy maltodextrins by means of two separate approaches. First, we consider the phenomenological model of Meares [14]. In this model, the activation energy for diffusion can be identified as the work against intermolecular forces of attraction of opening cylindrical holes having the diameter of the penetrant and the length equal to the length of the diffusion

* Corresponding author at: FrieslandCampina Research, Harderwijkerstraat 6, 7418 BA Deventer, The Netherlands. Tel.: +31 570 695902; fax: +31 570 695918.
E-mail address: gian.falco@hotmail.com (G.M. Falco).

¹ Current address: Procede Group Ltd, PO Box 328, 7500 AH Enschede, The Netherlands.

jump. Due to the large cohesive energy density induced by the strong hydrogen-bonds molecular interaction [15], Meares approach predicts in maltodextrins large activation energies for diffusion. The theory is combined with recent data [4,16] on the size and distribution of the intermolecular voids obtained from positron annihilation lifetime spectroscopy (PALS). We find that the jump length of the elementary diffusion step is consistent with the typical distance between hole volumes revealed by positron annihilation experiments. Moreover, we suggest that, by comparing the present data with new measurements of partially filled matrices, the Meares model could be used spectroscopically to determine which holes participate at most in the transport of molecules.

In a second approach, we apply the *transition state theory* [17] which has been quite successful in explaining the diffusion constant of small molecules in synthetic polymers [18]. The transition state theory is a microscopic theory with no fitting-parameters based on a short length scale description of the straining forces due to the intermolecular potentials. We find that the enhanced stiffness of the maltodextrin matrices is sufficient to reduce the diffusion constant of two or three order of magnitudes with respect to the typical synthetic materials. The predictions of the model for the diffusion of nitrogen in dry maltodextrins are compared with the limited data available in literature [2].

When transport occurs through the solution–diffusion mechanism, the diffusion is determined by the migration of adsorbed penetrant molecules inside the hole spaces of the matrix. Very little is known about the adsorption of nitrogen molecules in the cavities of the amorphous maltodextrinic matrices [2]. In Section 4, we tentatively address this problem. We calculate the gas sorption isotherms by means of the Kirchheim model [19]. This model includes the elastic distortion of the matrix during the sorption process. It can also be viewed as a generalization of the *Dual Mode Theory* [20], because it takes into account explicitly the broad size distribution of intermolecular hole cavities observed in positron annihilation experiments. In the case of nitrogen molecules in maltodextrins, the theory of Kirchheim predicts for the pressure–concentration isotherms strong deviations from the Henry's law even at relatively low pressures. This has to be ascribed to the enhanced shear modulus of maltodextrins and to the broad width of their hole volumes distributions. We are not aware of precise data on the solubility of nitrogen in glassy maltodextrins. Therefore, we have compared our results with the analogue curves obtained for typical low-free volume synthetic polymers in the same temperature range. Our conclusions are presented in Section 5.

2. Transport properties of low molecular weight compounds in glassy carbohydrate matrices

Diffusion of gases in polymers often follows Fick's law of diffusion [21] both in the rubbery and in the glassy state. Deviations from Fickian behavior are considered to be associated with the finite rates at which the polymer structure may change in response to the sorption or desorption of penetrant molecules [21]. In the case of maltodextrin matrices, however, many gases, including nitrogen, have a virtually negligible interaction with the matrix [2]. Therefore, the rate of diffusion is largely independent of the concentration and Fickian diffusion is then usually observed [2]. This holds true in particular at low penetrant concentration.

When the membrane is non-porous, gas permeation is commonly described in terms of a “solution–diffusion” mechanism

$$P = D \cdot S. \quad (1)$$

For polymers at temperatures $T \leq T_g$ not too far below the glass transition, molecular chain mobility tends to provide larger

and more frequent free-volume elements of sufficient size to accommodate diffusion steps of both large and small penetrant molecules. The diffusion constant is thus less sensitive to the penetrant size and the permeability is controlled by the variations of the solubility for molecules of different condensability. In low free-volume glassy polymers with low chain mobility ($T \ll T_g$) the frozen polymer chain restricts the redistribution of the free-volume. For penetrants to diffuse in glassy systems, they must jump from one region of the free-volume to another over an energy barrier. Hence the rate of permeation depends on the parameters which control the rate of diffusion such as the size of the penetrant. The variation of the solubility S turns out to be much weaker than the variations of the diffusion constant D . The breakdown of the free-volume theory below the transition region and the onset of a different mechanism is also indicated by a different slope of the curve for D [22,5]. Below the glass transition, the temperature dependence of the self-diffusion coefficient follows an Arrhenius law [22]

$$D = D_0 \exp(-E_d/RT), \quad (2)$$

where E_d is the activation energy for diffusion, D_0 is a constant and R is the universal gas constant. Typical values of the diffusion constant for small molecules in glassy synthetic polymers vary from $D_0 \sim 10^{-4} - 10^{-9} \text{ cm}^2/\text{s}$ [23]. Recent measurements [2] on nitrogen diffusion maltodextrin matrices below T_g at low water content report values for the diffusion coefficient down to $D = 10^{-12} \text{ cm}^2/\text{s}$.

The effects of the solubility on the permeation of small gases in polymer membranes can be estimated recalling that the solubility of small gases is closely related to their condensability. Gases with higher critical temperature T_c (more condensable) have lower solubility. Nitrogen (N_2) has a very low boiling point at $T_c = 77 \text{ K}$ lower than CO_2 ($T_c = 216 \text{ K}$), O_2 ($T_c = 91 \text{ K}$) or CH_4 ($T_c = 112 \text{ K}$). Therefore, the solubility coefficient in maltodextrins is expected to be lower for nitrogen than for other small penetrants. Unfortunately, we are not aware of any experimental data. Tentatively, we can use the solubility of nitrogen in Polysulfone (PSF) or in Polyvinylchloride (PVC). These polymers have respectively [24] $S \sim 0.3 \text{ cm}^3(\text{STP})/(\text{cm}^3 \text{ atm})$ and $S \sim 0.001 \text{ cm}^3(\text{STP})/(\text{cm}^3 \text{ atm})$.

With these values of D and S , from Eq. (1) we obtain a permeability of the order of

$$P \sim 10^{-5} - 10^{-7} \text{ barrer}, \quad (3)$$

where in SI units the barrer is defined as $1 \text{ barrer} = 3.348 \times 10^{19} \text{ kmol m}/(\text{m}^2 \text{ s Pa})$.

A comparison with Table 1 shows that the permeability coefficient of nitrogen in maltodextrins can be lower than in

Table 1

Diffusion, solubility and permeability of nitrogen measured in high-mobility rubbery polymers (Polydimethylsiloxane (PDMS) [41], Polyvinylidene chloride (PVdC) [42]), and glassy polymers (Polysulfone (PSF) [24], Polyvinyl chloride (PVC) [42,43], Polyvinyl alcohol (PVA) [44], Ethylene Vinyl Alcohol (EVOH) [45]). The solubility coefficient for the PVC has been calculated from the permeability [42] and the diffusion constant [43] in this table by means of Eq. (1). The permeability is measured at the following temperatures, 298 K (PDMS, PVC), 296 K (EVOH), 303 K (PVdC), 308 K (PSF).

Polymer	D (cm^2/s)	S ($\text{cm}^3(\text{STP})/\text{cm}^3$ poly. atm)	P (barrer)
PDMS	2.9×10^{-5}	0.9×10^{-1}	3.5×10^2
PVdC	–	–	$0.9 \cdot 10^{-3}$
PSF	0.9×10^{-8}	1.9×10^{-1}	2.2×10^{-1}
PVC	2.2×10^{-9}	4.4×10^{-2}	1.3×10^{-2}
PVA	–	–	$\sim 1.0 \times 10^{-5}$
EVOH	–	–	$6.1 \times 10^{-6} - 2.4 \times 10^{-5}$

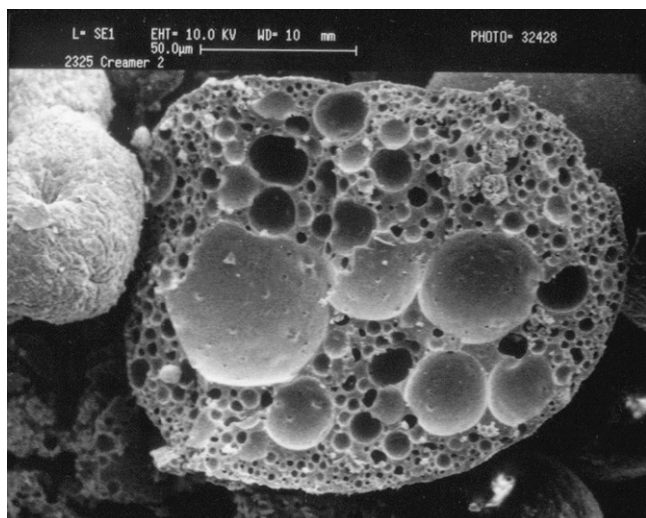


Fig. 1. SEM picture of the cross-section of a maltodextrin powder particle containing stored pressurized gas inside the voids. Such powders are commercially available and have been found to lose little gas over the course of a year [11–13].

typical synthetic low-free volume glassy polymers. Among the examples considered there, Polyacrylonitrile (PAN), which has the lowest permeability [25], has a fractional free volume ($ffv \approx 5\%$) comparable with that of maltodextrins. Polyvinylchloride, which can be considered very representative of synthetic polymer, has a fractional free volume $ffv \approx 15\%$.

The permeability found in Eq. (3) can be used in order to estimate the storage stability of nitrogen in maltodextrin powders [13]. It was recently found that nitrogen gas can be stored at a pressure of around 30 bar inside voids in powder particles consisting of maltodextrin with little gas loss for over one year [11,12]. A Scanning Electron Microscope (SEM) picture of the cross-section of a maltodextrin powder particle is shown in Fig. 1. In a simplified but realistic model [13], we can assume the gas forming a 30 bar pressure spherical bubble with area $A = 100 \mu\text{m}^2$ surrounded by a shell with a thickness of $\Delta x = 10 \mu\text{m}$. By assuming a permeability of $P \sim 10^{-7}$ barrer, the flux of particles $J = PA\Delta p/\Delta x$ through the surface is of the order of $J = 10^{-17} \text{cm}^3/\text{s}$. Since the bubble contains around 10^{-8}cm^3 of gas, it takes around 100 days for the bubble to empty in correspondence with the storage stability in practice [11–13]. Therefore, the permeability of nitrogen in maltodextrin at 30 bar is expected not to exceed this value. The main goal of our study is to understand to what extent the traditional solution–diffusion model for transport of small gases in glassy polymers can explain the remarkably high stability of pressurized nitrogen encapsulated in maltodextrin. To this purpose, we consider a semi-quantitative approach based on some traditional solution–diffusion theories. Although the cause of this paper concerns the rather specific topic of gas encapsulation in a glassy carbohydrate matrix, the more general phenomenon of the permeation of small solutes through glassy carbohydrates is of great importance for food and pharmaceuticals [6–9].

3. Theories of diffusion of (small) gas particles in glassy polymers

3.1. The model of Meares

Low free-volume, rigid, glassy polymers have very restricted chain motion. This implies that small free-volume elements,

suitable for diffusion steps of small gases, occur much more often than free-volume elements large enough to allow diffusion of larger gas molecules. The large disparity in the availability of free volume elements leads to strong dependence of D on penetrant size. This experimental fact was the main feature considered by Meares [14] in his phenomenological model. According to Meares, the activation energy for diffusion in Eq. (2) behaves linearly with the square of the penetrant diameter d . That is, the elementary diffusion step is not governed by the energy necessary to create a hole that can accommodate the penetrant molecule, but by the energy required to separate polymer chains so that a cylindrical void is produced which allows the penetrant to jump from one equilibrium position to another. The relation proposed by Meares follows from the work against the internal pressure required for the penetrant to push through a neck with given radius equal to that of the penetrant

$$E_D = \int^V p dV. \quad (4)$$

Since the internal pressure in a liquid corresponds approximately to the cohesive energy density ε in a cylindrical geometry we have

$$E_D = (\pi/4)d^2 N_A \lambda \varepsilon, \quad (5)$$

where N_A is the Avogadro's number, λ is the cylindrical void jump length. The structure and rigidity of the polymer strongly affects the mobility of gases through the dependence on the cohesive energy density ε [26,15]. The higher the cohesive energy the more difficult for the penetrant to push through the neck.

The cohesive energy density is related to the Hildebrand solubility parameter δ through the relation

$$\varepsilon = \delta^2. \quad (6)$$

Maltodextrins are highly water soluble. The cohesive energy for highly water soluble polymers can be estimated because for a solid to dissolve in a liquid the solubility parameter must be close to the solubility parameter of the liquid, which in case of water is $\delta \sim 47.8 \text{ (MPa)}^{1/2}$. More quantitative calculations based on group contribution methods in Ref. [27] confirm this picture. They find

$$\varepsilon \sim 1.6 \text{ kJ/cm}^3, \quad (7)$$

which corresponds to a solubility parameter $\delta \sim 40 \text{ (MPa)}^{1/2}$. Table 2 gives an overview of solubility parameters and cohesive energies for several polymers. It can be seen that generally the higher the ability of a polymer to form hydrogen bonds the larger its solubility parameter and its cohesive energy density. Of the shown polymers, maltodextrin has the largest cohesive energy, much larger than that of synthetic polymers. From the point of

Table 2

Hildebrand solubility parameter and cohesive energy densities of some typical synthetic rubbery polymers (Polyethylene (PE), Polyethylene oxide (PEO)) and glassy polymers (Polypropylene (PP), Polystyrene (PS), Polycarbonate (PC), Polysulfone (PSF), PVC, and PVA). The data for δ are taken from [46] (PP, PVC), [47] (PE, PS), [15] (PC), and [42] (PSF, PVA, PEO). The glass transition temperature data are taken from [48] (PE, PP, PS, PC, PVC, PVA) and from [42] (PSF, PEO).

Polymer	$\delta \text{ (MPa)}^{1/2}$	$\varepsilon \text{ (kJ/cm}^3\text{)}$	$T_g \text{ (K)}$
PE	16.2	0.261	93–193
PEO	20.2	0.408	232
PP	16.6	0.275	273
PS	18.3	0.333	368
PC	20.6	0.426	418
PSF	20.3	0.410	459
PVC	19.5	0.380	353
PVA	25.8	0.664	358

view of Meares theory this means that higher activation energies for diffusion are expected.

The Meares model, however, cannot be used to make a priori predictions of the activation energy. Therefore, Eq. (5) can be better interpreted as a scaling relation between the activation energy for diffusion and the cohesive energy density of the polymer matrix times the square of the gas diameter. More recent studies on the permeability–selectivity correlations in polymeric gas separation membranes [28,29] confirm the conceptual validity of Meares scaling hypothesis. Nevertheless, the dependence of diffusion on the polymer chemical structure, represented by its cohesive energy density, is only one of the determining factors of the membranes properties. The physical structure of the polymer such as hole volume, mobility and order have also a strong bearing on its barrier properties. In Meares scaling approach, the mechanical structure of the polymer is described by a length scale, the jump length λ , which follows naturally from dimensional considerations in Eq. (5). Unfortunately, the jump length λ cannot be related to macroscopic parameters of the polymer matrix. For this reason, it has been applied in the past to synthetic polymers as a fitting parameter. Only recently, Alentiev and Yampolskii [26] have combined the Meares scaling hypothesis with the information from positron annihilation lifetime experiments. The analysis of spectroscopic positron annihilation data of the hole volumes in a series of glassy synthetic polymers, indicates the existence of a characteristic length scale related to the typical distance between neighboring free volume elements. They find that, for a large class of glassy polymers, this characteristic length is in reasonable agreement with the diffusion jump lengths estimated from the Meares formula using the data for the diffusional activation energies [26].

By reversing this argument, we will use recent positron annihilation data [16] in order to estimate λ and thus calculate a lower boundary for the activation energy of diffusion of nitrogen in maltodextrin. The determination of λ goes as follows. The specific volume of dry maltodextrin is about $v_{sp} \sim 0.650 \text{ cm}^3/\text{gr}$ [4], while the free volume is estimated to be $v_f \sim 0.04 \text{ cm}^3/\text{gr}$. Therefore, the fractional free volume is

$$ffv \sim 6\%. \quad (8)$$

In synthetic polymers, such a low value of the fractional free volume occurs only in a restricted class of densely packed glassy polymer such as Polyacrylonitrile (PAN) or Polyvinyl alcohol (PVA). Remarkably, positron annihilation measurements do not only allow to calculate the ffv but they also deliver information about the distribution of the hole volumes. By assuming that the number of holes is independent of the composition of the maltopolymer–maltose blends, the number density of holes for a generic anhydrous maltopolymer–maltose compound has been estimated in Ref. [16] as

$$v_h \simeq 7.6 \times 10^{20} \text{ g}^{-1}. \quad (9)$$

Therefore, the density of holes per unit volume can be deduced from the relation

$$n_h = v_h/v_{sp} \simeq 1.15 \times 10^{21} \text{ cm}^{-3}. \quad (10)$$

If one cubic centimeter of the polymer contains $N \simeq 1.15151 \times 10^{21}$ free volume elements, the average volume available for single volume element is

$$\Delta V \simeq 0.86 \times 10^3 \text{ \AA}^3. \quad (11)$$

The size

$$L \simeq 9.5 \text{ \AA}, \quad (12)$$

of the average cubic volume cell available for single free volume element, determines the on-average distance between two

neighboring hole elements and should be correlated to the jump length λ . In the simplest model, the jump length can be related to the size L through the relation

$$\lambda \sim L - 2r_h, \quad (13)$$

where, assuming spherical symmetry, r_h is the radius of the typical hole volume element. The most recent data obtained from positron annihilation experiments report for maltodextrins at low water content at $T=298 \text{ K}$ indicate that the average hole volume size is [16]

$$r_h \simeq 1.71 \text{ \AA}. \quad (14)$$

Note that the average size of the hole volumes is smaller than the size of the nitrogen molecule. This characteristic, which is typical for dry maltopolymers, does not generally occur in synthetic polymers, where values of $r_h \geq 2 \text{ \AA}$ have been reported [30]. An exception may be represented by extremely densely packed low-free volume polymers with fractional free volume below the 5%. By inserting the result of Eq. (14) into Eq. (13) we obtain $\lambda \simeq 6 \text{ \AA}$ and Meares formula of Eq. (5) yields an activation energy $E_D \simeq 66 \text{ kJ/mol}$.

However, the value of Eq. (14) represents only the average size, while the hole volume size is Gaussian distributed [16] around the mean value with variance $\sigma_{r_h} \sim 0.5 \text{ \AA}$ as shown in Fig. 2. It is likely that not all the cavities participate in the diffusion process, but only the holes which are big enough in order to accommodate a nitrogen molecule of diameter $d_{N_2} \simeq 3.79 \text{ \AA}$. If we assume that only holes with $r_h \geq d_{N_2}/2$ participate in diffusion we need to eliminate the holes with radius smaller than the nitrogen molecular radius $d_{N_2}/2 = 1.82 \text{ \AA}$. The average distance between these hole centers is thus larger than the above estimated value of L , the effective size of the available volume per hole is thus increased to $L_{\text{eff}} \simeq 13.4 \text{ \AA}$ and the jump length to $\lambda \simeq 10 \text{ \AA}$. This leads to an increase of the activation energy up to $E_D \sim 109 \text{ kJ/mol}$. An analogous effect would occur when we consider a penetrant with bigger size, because a larger molecule has lower probability of finding in its vicinity a hole of suitable size. Our results for the activation energy can be compared with value estimated by Schoonman et al. [2]. From the temperature dependence of the measured diffusion constant they find $E_D \sim 70 \text{ kJ/mol}$, which is within the range of our lower and upper estimated values.

Since our estimation of the lower limit activation energy is based on a scaling approach, it cannot be considered a rigorous result. Nevertheless, it can be fully appreciated if we compare these energies with the typical activation energies measured for diffusion of small gases in glassy synthetic polymers. In PVC, for example, the value $E_D \simeq 31 \text{ kJ/mol}$ has been found. Therefore, we can conclude that the enhanced activation energies occurring in maltopolymers are thus due to the high cohesive energy induced

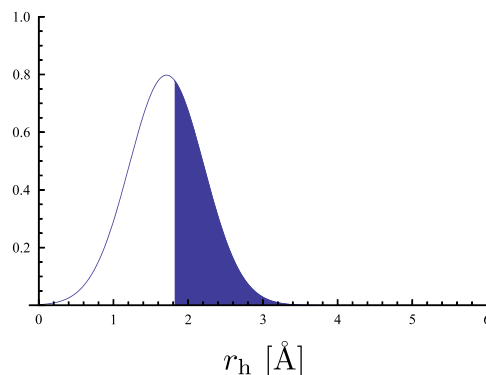


Fig. 2. Distribution of the hole volume size [16] in for a pure maltopolymer sample ($\phi_m=0$) at low water activity $a_w=0.33$. In the shaded region the hole with radius larger than the nitrogen molecule radius are shown.

by the hydrogen bonds and to the reduced size of the characteristic hole volumes. Unfortunately, a high cohesive energy implies for maltodextrins also a high solubility in water. Therefore, their characteristic ability to act as a barrier is easily lost in a wet environment due to the disruption of hydrogen bonds.

3.2. The transition state theory

Below the glass transition, the polymer motions become restricted and the unoccupied volume becomes fixed. In order for penetrants to diffuse in such a glassy system, they must jump from cavity to cavity through the opening of a neck that arises due to thermal motions of the glassy polymer.

There is likely to be a significant activation energy for these jumps, and indeed such barriers have been observed in molecular dynamics simulations. Simulations [31] show evidence that oxygen molecules are rattling around for long periods in cavities. Occasionally, a neck to a neighboring cavity opens and the penetrant may jump through it. The size and the frequency of these jumps seems to correlate with the size of the penetrant and the nature of the polymer. The smaller the penetrant and the more rubbery the polymer, the more frequently jumps occur. As would be expected, D 's for smaller penetrants are also larger. In general, for synthetic polymers the jump length found varies from 2 to 20 Å.

In general there is a wide distribution of jumps. However, in order to calculate D , one needs to postulate an *average, rate-determining* typical jump. The coefficient D is taken from the slowest jump and not the average of all the jumps. The reason is that faster jumps are effectively slowed down, since their reverse jumps will also be as likely to occur, roughly speaking, inhibiting diffusion. The slowest jumps, being rare, are likely to occur in isolated instances, implying that they are the critical jumps to net penetrant displacement. We assume that penetrants execute these jumps in a random manner as in a random walk. By stochastic theory, the diffusion coefficient is given by

$$D = k\ell^2/6. \quad (15)$$

When the motion is dominated by rare activated events, *transition state theory* [17,32,33] is a suitable approach to model the behavior. For chemical reactions, the energy barrier is due to the breaking of chemical bonds, for jumps, the energy barrier is due to straining forces induced by the molecular potentials. In this way the transition state theory framework describes the polymer matrix by a series of macrostates, each corresponding to a system configuration at each potential minimum. The diffusive jump of a penetrant can then be modeled as a first order reaction with rate constant k where the penetrant jumps from one macrostate to another. Upon each jump the penetrant passes through the transition state: the highest energy barrier on the lowest energy pathway to the neighboring macrostate [34]. The rate coefficient for the jump is obtained from the transition state theory formula

$$k = \frac{k_B T Q^+}{h Q} \exp\left[-\frac{E_0}{k_B T}\right], \quad (16)$$

where h is the Planck's constant, Q^+ and Q are the partition functions of transition state (the neck) and reactant (the cavity) respectively, and E_0 is the difference in energy between reactant and transition state minima. Using transition state theory this way, Gray-Weale et al. [18] successfully predict the diffusion coefficients of simple gases, small hydrocarbons and alcohols in glassy poly(vinyl chloride) over a wide range of values of experimental diffusion coefficients. Although the model is untested for maltodextrins, the ratio of the partition functions Q^+/Q of the

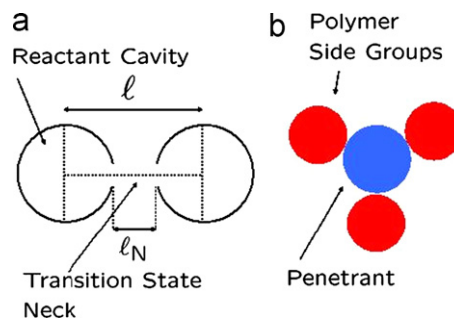


Fig. 3. (a) Illustration of the geometry of the reactant cavity and the transition state neck. (b) The picture shows the trigonal arrangement in the transition state of the side groups components of glucose, namely oxygen atoms (red smaller spheres), around the penetrant nitrogen molecule (blue larger sphere). Note that the reactant state would have four of the side groups arranged tetrahedrally. (For interpretation of the references to color in this figure caption, the reader is referred to the web version of this paper.)

transition state and of the reactant state respectively is evaluated as in Ref. [18]. This implies that the transition state has three groups arranged trigonally (see Fig. 3(b)) and the reactant state has four groups arranged tetrahedrally, as successfully applied for small non-polar penetrants in poly(methyl methacrylate) in the glassy regime [35]. In order to make the paper self-contained some details are given in Appendix A.

The jump length ℓ is the displacement of the penetrant in jumping from one cavity to another cavity through some neck pushing apart some part of the polymer chain. The geometry of the model is shown in Fig. 3(a). Transition state simulations indicate that most jumps occur through the polymer's side groups. We treat the polymer side group components atoms as hard spheres with diameter given by the Lennard-Jones diameter. In the case of maltodextrin, a polymer consisting of glucose ($C_6H_{12}O_6$) monomers, the penetrant would be typically surrounded by hydrogen and oxygen atoms. Since the latter are much bigger, the neck's length ℓ_N is taken as the diameter of the oxygen atom σ_a . Moreover, the jump length goes from the center of the penetrant in the reactant cavity to that in the product cavity. Therefore, the thickness of the penetrant σ_b also needs to be included in the jump length (see Fig. 3(a))

$$\ell = \sigma_b/2 + \sigma_a + \sigma_b/2. \quad (17)$$

In the case of nitrogen molecules (N_2) we have $\sigma_b = 3.79$ Å and the jump length is $\ell \simeq 7.0$ Å.

The energy E_0 is the difference in energy on the system potential energy surface between reactant and transition state. The components of E_0 are harmonic bends and stretches, three-fold torsional potentials and non-bonded Lennard-Jones potentials. The activation energy E_0 is given by the minimum of the potential function

$$U(r) = \frac{N_A \pi l_0 (r^2 - r_0^2)}{10^3 \rho} + 12\varepsilon \left[\left(\frac{\sigma}{r}\right)^{12} - \left(\frac{\sigma}{r}\right)^6 \right], \quad (18)$$

where $r' = r + \sigma_a/2$ is the distance between glucose side group atoms and penetrant atoms. The variables σ and ε are obtained using the standard Lorentz-Berthelot mixing rules $\sigma = \sigma_a + \sigma_b$ and $\varepsilon = \sqrt{\varepsilon_a \varepsilon_b}$. The transition is situated at the top of the lowest energy path connecting two minima.

The first term of the potential in Eq. (18) defines the energy required for the polymer to form a cylindrical neck with radius r and length l_0 . The isothermal compressibility $\rho = -(1/V)(\partial V/\partial p)_T$ occurs because forming a neck is a cooperative process involving small contributions from many atoms rather than having one moving by itself. If a neck of radius $r < r_0$ needs to be formed, no

energy is required since r_0 is the radius of the pre-existing neck in the reactant state [36]. The factor of $10^{-3}N_A$ is introduced to convert this kJ mol^{-1} . For maltodextrins, the length l_0 is approximated with the Lennard–Jones diameter of an oxygen atom.

The second term describes the competing mechanism of the penetrant trying to squeeze through the neck, which is due to the change in non-bonded Lennard–Jones interactions between the penetrant and polymer atoms. The larger the neck becomes, the less the penetrant has to be squeezed, until the neck is so wide that the penetrant does not have to be squeezed at all, at which point, the potential energy equals zero.

The model assumes that the transition state neck for the average jump is made of three glucose atoms arranged symmetrically as shown in Fig. 3(b). The assumption is then made that the difference in penetrant–polymer non-bonded energy in taking the penetrant from reactant to the neck in the transition state is due to the repulsive interactions between the penetrant and these three side components of the glucose molecule, namely hydrogen or oxygen atoms. Since the latter are much bigger the interaction will be dominated by the interaction between N_2 and O atoms. The assumption will only hold when the neck is less than the Lennard–Jones diameter of the penetrant. Otherwise, these repulsion interactions will be small, making other energy changes such as those in attractive energy interactions important. In Fig. 4 the potential function $U(r)$ at room temperature $T=298\text{ K}$ experienced by N_2 molecules in maltodextrin (DE 12) at low water activity $a_w=0.22$ (red line), is compared with the potential in glassy PVC (blue line). This material has been chosen because it represents a typical low free-volume synthetic polymer. The Lennard–Jones parameters for chloride atoms are $\sigma_a=3.40\text{ \AA}$ and $\varepsilon_a=0.994\text{ kJ/mol}$ [18]. For maltodextrin we have taken the parameters of the oxygen atoms $\sigma_a=3.20\text{ \AA}$ and $\varepsilon_a=0.837\text{ kJ/mol}$ as discussed above. Nitrogen parameters are $\sigma_b=3.79\text{ \AA}$ and $\varepsilon_b=0.590\text{ kJ/mol}$. With these values, the upward shift of the potential minimum for maltodextrins is to ascribe to the enhanced rigidity of the maltodextrin polymer chain with respect to the synthetic compound. At room temperature, the compressibility of PVC, $\varrho=2.65\times 10^{-10}\text{ Pa}^{-1}$ [18] is about three times larger than that of maltodextrins which is $\varrho=1.17\times 10^{-10}\text{ Pa}^{-1}$ [4]. The role of the compressibility is clearly elucidated in the inset of Fig. 4. There, the dependence of the activation energy E_0 on the compressibility of maltodextrins, when keeping the other parameters fixed, is shown. Analogously, the effects of the compressibility on the diffusion

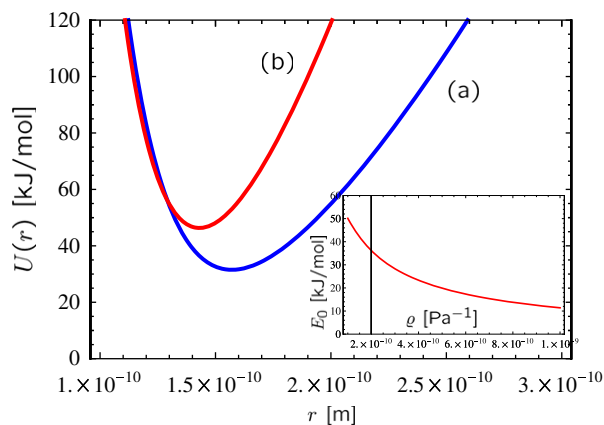


Fig. 4. Potential function $U(r)$ of Eq. (18) for diffusion of nitrogen molecules at room temperature $T=298\text{ K}$ in glassy PVC (blue line (a)) and low water activity maltodextrin DE-12 (red line (b)). The minimum of the potential function $U(r)$ represents the activation energy E_0 of Eq. (16). The dependence of this minimum on the compressibility ϱ is shown in the inset for the range of compressibilities at different water activities considered in Ref. [4]. (For interpretation of the references to color in this figure caption, the reader is referred to the web version of this paper.)

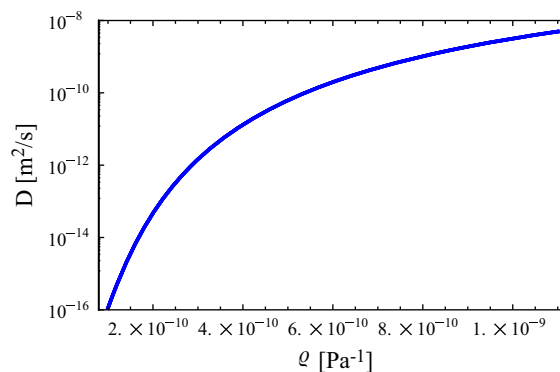


Fig. 5. Diffusion coefficient of N_2 in glassy maltodextrins as function of the compressibility. The parameters of the maltodextrin are taken the same as in Fig. 4.

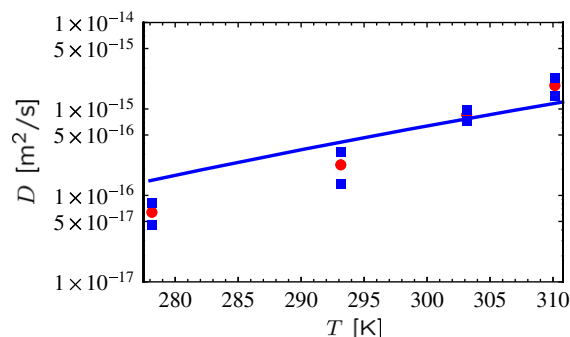


Fig. 6. Prediction of the transition state theory for the diffusion coefficient of N_2 in glassy maltodextrins as function of the temperature (solid blue line). The red circles indicate the values found experimentally in Ref. [2] for the diffusion coefficient D of N_2 in maltodextrin DE 11–14 at water activity $a_w=0.23$. The blue squares indicate here the range of the experimental error. (For interpretation of the references to color in this figure caption, the reader is referred to the web version of this paper.)

constant D are described in Fig. 5. We see that a reduction in compressibility as from typical values of maltodextrins to PVC is sufficient to reduce the value of the diffusion constant by three or four order of magnitudes. We have tested this prediction with the data of Schoonmann et al. [2] for the diffusion constant of nitrogen molecules in maltodextrin DE 11–14 at water activity $a_w=0.23$ measured at different temperatures. The results are shown in Fig. 6. The agreement between the transition state theory (blue line) and the experimental values (red dots) is not between the experimental error (blue dots) but the curve reproduces quantitatively well the strong suppression of the diffusion occurring in maltodextrins. Note that, in deriving this result, we have assumed that the compressibility remains constant at $\varrho=1.17\times 10^{-10}\text{ Pa}^{-1}$ [4] along the narrow range of temperature considered in the experiment of Schoonmann et al.

4. Kirchheim's sorption model for nitrogen gas molecules in maltodextrins

Below the glass transition, the non-equilibrium nature of the glassy state complicates our understanding of the sorption process. The sorption of gases in glassy polymers is highly non-linear even at low penetrant activities and deviates strongly from Henri's law. Gas sorption isotherms exhibit a characteristic shape which is concave to the pressure axis. When this behavior is observed, the most widely used model to fit gas sorption data in glassy polymers at low to moderate pressures is the dual sorption model [20]. It assumes the existence of two populations of

penetrant molecules in equilibrium within the glassy polymer. Next to the Henry's law population absorbed by ordinary dissolution there is another occupying the preexisting gaps frozen into the glassy polymers as it was cooled below the glass transition temperature.

The dual-sorption model is widely used to fit gas sorption data but is not very useful to make a priori predictions. Unfortunately, we are not aware of precise data on the solubility of nitrogen in glassy maltodextrins. Moreover, while the dual-sorption model is based on a two-(energy) level system, the broad distribution of the intermolecular spaces revealed in positron annihilation experiments in glassy maltodextrins [16], suggests that a distribution of site energies would be more appropriate. Such a description has been proposed by Kirchheim [19] for the sorption of small molecules in glassy synthetic polymers. In the theory of Kirchheim sorption occurs within a variety of sites belonging to the free volume providing different space for the dissolved species. He considers a Gaussian distribution of the hole-volumes V_h as derived long ago by Bueche [37]

$$f(V_h) = f_0 \exp[-B_g(V_h - V_{h0})^2 / 2V_{h0}RT_g], \quad (19)$$

where with f_0 we denote a numerical prefactor, V_{h0} is the average hole volume, $B_g = 1/\rho_g$ is the bulk modulus at the glass transition temperature T_g , and R is the gas constant. The microscopic parameters occurring in Eq. (19) are generally known for maltodextrins [4,16]. Positron annihilation experiments [16], however, show that the hole volume distribution deviates from a Gaussian function being skewed at large values. Despite this, in the following, we will approximate the true asymmetric distribution with the distribution Eq. (19), because this should not affect qualitatively the shape of the sorption isotherms. The effects of the skewness of the distribution will be discussed apart.

Beside the nearest neighbor interaction between the molecule and the segment of the polymer during the sorption process, the theory of Kirchheim includes the elastic distortion of the matrix. If the size of the small molecule is larger than the size of the hole, the glassy polymer is elastically distorted during the sorption of the solute molecule. The corresponding elastic energy is given by [38]

$$G_{el} = \frac{2}{3} B_s \frac{(V_g - V_h)^2}{V_h}, \quad (20)$$

where $B_s \approx B/(2+2\nu)$ with $\nu = 1/3$ for the glassy state is the shear modulus at temperature T , and V_g is the van der Waals volume of the solute molecule. Eqs. (19) and (20) imply a Gaussian distribution for the free energy G of dissolution of molecules into the holes of a glassy polymers [19]

$$n(G) = (1/\Sigma\sqrt{\pi}) \exp[-(G-G_0)^2/\Sigma^2], \quad (21)$$

where the width is

$$\Sigma = \frac{2(V_g^2 - V_{h0}^2)B_s}{3V_{h0}^2} \sqrt{\frac{2RT_g}{BV_{h0}}}. \quad (22)$$

The average free energy G_0 corresponds to the free energy of one solute molecule in an average hole with volume V_{h0} of the glassy polymer. A permanent dipolar moment decreases G_0 and increases the solubility. The polarizability of a small molecule is measured by the Lennard-Jones force constant. Therefore, there is a correlation between the Lennard-Jones parameter and the solubility of small molecules.

Since the Lennard-Jones potential of the gases describes melting and evaporation of gases, G_0 correlates also with the boiling point [39,40]. For gases having the same molecular volume, where the elastic part of G_0 is similar, the correlation is mainly due to the enthalpy of dissolution which increases with decreasing

condensation temperature of the gas. Therefore, a high dissolution enthalpy is expected for nitrogen because, nitrogen has the lowest condensation temperature after helium atoms. This is well known for sorption in synthetic glassy polymers [19], where the dissolution enthalpy of nitrogen molecules is narrowly distributed around $G_0 = 25$ kJ/mol [19]. Since maltodextrins are characterized by an extreme low free-volume and a very low compressibility, it is reasonable, in absence of specific data, to consider $G_0 = 25$ kJ/mol as a lower bound.

The total solute concentration can be calculated from the distribution of the free-energy of dissolution by assuming that the thermal occupancy of the holes follow the Fermi-Dirac statistics

$$c = \int_{-\infty}^{\infty} n(G) \frac{1}{1 + \exp(G-\mu)/RT} dG. \quad (23)$$

The chemical potential μ of the dissolved gas is related to the gas pressure p by the relation

$$\mu = \mu_0 + RT \ln p, \quad (24)$$

where μ_0 is the standard value of the dissolved molecules in the gas phase at 1 atm. In order to transform the concentration (23), which is defined as fraction of sites being occupied, into the usual unities given as $\text{cm}^3(\text{gas})/\text{cm}^3(\text{polymer})$, we have used the data from positron annihilation experiment for the number n_h of sites per cm^3 polymer defined in Eq. (10).

The prediction of Eqs. (23)–(24) for the pressure-concentration isotherms for nitrogen ($V_g \approx 46 \text{ \AA}^3$) are shown in Fig. 7. The blue line describes the isotherm of glassy PEMA at 308 K [19]. PEMA has a glass transition temperature at 334 K, the average hole volume is $V_{h0} \approx 43 \text{ \AA}^3$ and a hole density $n_h = 6.7 \times 10^{21} \text{ cm}^{-3}$. At T_g it has a bulk modulus $B = 2.5 \times 10^9$ Pa and $B = 3.0 \times 10^9$ Pa at $T = 308$ K in the glassy state. Similar values are typical of many other synthetic glassy polymers. For this set of parameters the condition $-(\mu - G_0) \gg \Sigma^2/4RT$ holds and from Eqs. (23) to (24) Henry's law $c \propto p$ for an ideal solution of molecules is recovered. This limit is characteristic of the high temperature regime in the rubbery or liquid state. There the shear modulus becomes several order of magnitudes smaller than in the glassy state and the Gaussian distribution becomes a Dirac- δ function. Then, at $c \ll 1$, Eq. (23) reproduces the Henry's law $c = p \exp[(\mu_0 - G_0)/RT]$.

As we have seen in a previous section, glassy maltodextrins ($T_g \approx 403$ K) at room temperature have a large bulk modulus, $B = 8.5 \times 10^9$ Pa. Nevertheless, due to the temperature dependence of the bulk modulus which decreases down to $B_{Tg} = 5.5 \times 10^9$ Pa [4]

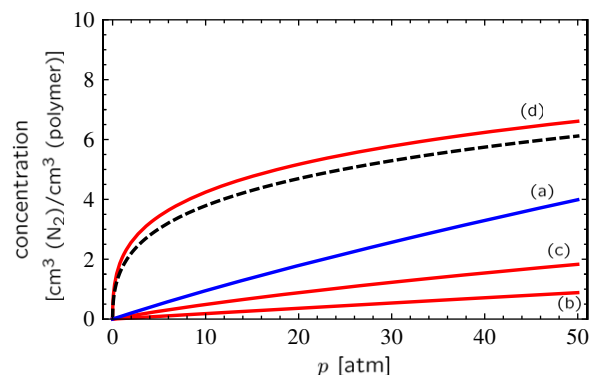


Fig. 7. Prediction of the Kirchheim theory (Eqs. (23)–(24)) for the pressure-concentration isotherms for N_2 in glassy PEMA at $T = 308$ K (blue line (a)) [19] and glassy maltodextrin (red lines): (b) $T = 373$ K, (c) $T = 353$ K, (d) $T = 298$ K. The dotted (black) line indicates the analytical result of Eq. (25) for $T = 298$ K. (For interpretation of the references to color in this figure caption, the reader is referred to the web version of this paper.)

when increasing the temperature near the glass transition, Henry's law behavior is found as well for temperatures well above 298 K. This is illustrated in the straight red lines of Fig. 7 taken at $T=353$ K and $T=373$ K with $B=6.6 \times 10^9$ Pa and $B=5.5 \times 10^9$ Pa respectively [4]. The other parameters are [4] $V_{ho} \simeq 48 \text{ \AA}^3$, $n_h \simeq 1.16 \times 10^{21} \text{ cm}^{-3}$ at $T=353$ K and $V_{ho} \simeq 55 \text{ \AA}^3$, $n_h \simeq 1.14 \times 10^{21} \text{ cm}^{-3}$ for $T=373$ K. In both cases, the condition $-(\mu-G_0) \gg \Sigma^2/4RT$ is satisfied.

The situation is different at room temperature where the maltodextrins are deeply into the glassy state. The isotherm is described by the curved red line of Fig. 7, where we have used also that $V_{ho} \simeq 39 \text{ \AA}^3$, and $n_h \simeq 1.17 \times 10^{21} \text{ cm}^{-3}$. Due to the large bulk modulus the free-energy distribution spreads over a broad range and the condition $-(\mu-G_0) \ll \Sigma^2/4RT$ holds. In this limit, of broad distributions and low temperatures, the Fermi-Dirac distribution degenerates to a step function and the integration of Eq. (23) can be performed analytically yielding

$$c = \frac{1}{2} + \frac{1}{2} \text{Erf} \left[\frac{\mu-G_0}{\Sigma} \right]. \quad (25)$$

The isotherm calculated with Eq. (25) is illustrated in the dashed line of Fig. 7. It approximates very well the result of Eq. (23) because, due the broad distribution induced by the large bulk modulus, the sorption takes place deeply in the non-linear regime $-(\mu-G_0) \ll \Sigma^2/4RT$. Since this regime is generally difficult to reach in synthetic polymers [19], it should be straightforward to test Kirchheim's theory in laboratory using maltodextrins.

Moreover, the two limits of the model correspond to two distinct filling mechanisms [19] which could be investigated in positron annihilation experiments. When Henry's law applies, molecules are not saturating low energy sites but they gain configurational energy by occupying high energy sites. Differently, for broad distributions and low temperatures, minimization of the free energy proceeds from occupying sites with the lowest energy possible only. This picture could be tested by means of positron annihilation data on hole volume distributions of partially filled maltodextrin matrices.

Few approximations have been introduced in order to derive our results. First, the equilibrium concentrations of Fig. 7 have been calculated with the lower boundary value for the dissolution enthalpy G_0 discussed above. Increasing the value of G_0 would lead to a shift downwards of the concentration isotherm, and, in the linear regime, to a lower solubility. However, we are not aware of measurements of either the solubility S of G_0 for nitrogen in maltodextrins and no definite conclusion can be drawn. Second, the width of the hole distribution we have considered at Eq. (19) seems to underestimate the width calculated from positron annihilation experiment. Moreover, as anticipated above, the distributions observed experimentally deviates from a Gaussian being skewed at large values. While increasing value of the width of the hole volume distribution and thus of Σ , enhances the curvature of the isotherms, the effects of the skewness at large values should be to provide more space for solvation. However, it is difficult to quantify this aspect more precisely.

From the slope of the concentration isotherms of Fig. 7 the solubility can be estimated by means of the relation $S(p) = dc/dp$. The values obtained for the solubility of nitrogen in maltodextrins at 30 bar is about $S \simeq 3 \times 10^{-3} \text{ cm}^3(\text{STP})/(\text{cm}^3 \text{ atm})$. By combining this result with the estimation of the diffusion constant calculated from the transition state theory $D \sim 10^{-12} \text{ cm}^2/\text{s}$, we obtain a permeability of about $P \sim 10^{-7} \text{ bar}$ in agreement with the value used in the derivation of the storage time in maltodextrin powders of Section 2.

5. Conclusions

The sorption and diffusion of nitrogen in glassy maltodextrins at low water content has been investigated within the framework of the solution-diffusion model for transport of small molecules. The interplay between the small free-volume available and the enhanced bulk-modulus, has been analyzed by means of a direct comparison with typical low free-volume synthetic polymers in the same temperature range. We have found that both the processes of sorption and transport are strongly affected by the reduced hole-volume characteristic size and by the rigidity induced by the strong intermolecular hydrogen-bond interactions of the carbohydrate matrices. This leads to diffusion constants that are exceptionally low when compared with the diffusion constants for gases in synthetic polymers.

While our semiquantitative results confirm the excellent barrier properties observed in amorphous carbohydrates, more experimental input is needed in order to test the assumptions and to improve quantitatively the approach presented here. Future positron annihilation lifetime studies on the microscopic structure of the voids inside the glassy matrices could be of primary importance in order to accomplish this goal.

Appendix A. The partition function for the average jump

The partition function Q^+/Q , can be calculated as product of different components. This model assumes that both Q^+ and Q can be broken up into three components each, one due to penetrant, q_{pen} , one due to the maltodextrin, q_{po} , and one due to the interaction between penetrant and maltodextrin, q_{pepo} . Therefore, we have

$$\frac{Q^+}{Q} = \frac{q_{pen}^+ q_{po}^+ q_{pepo}^+}{q_{pen} q_{po} q_{pepo}}. \quad (A.1)$$

The penetrant is treated with no internal degrees of freedom that means $q_{pen}^+ = q_{pen} = 1$. The pure maltodextrin contribution q_{po}^+/q_{po} is expected to be slightly less than 1, since the maltodextrin will be more constrained in the transition state. However, we take $q_{po}^+/q_{po} = 1$ as in Ref. [18].

The penetrant-maltodextrin partition functions is calculated for a neck consisting of three side group atoms of the glucose molecule tetrahedrally arranged around the penetrant molecule. The force constant λ , of the harmonic potential is given by the second derivative of the potential, taken to be n Lennard-Jones potentials,

$$\lambda = J \frac{4\epsilon\sigma^6}{r^8} \left[\frac{156\sigma^6}{r^6} - 42 \right], \quad (A.2)$$

where J is the number of nearest-neighbor atoms and r is the distance between penetrant and maltodextrin atoms. The frequencies of vibrations are obtained by the equation $\nu_i = \sqrt{\lambda_i/m}/2\pi$, where m is the mass of the penetrant. In the reactant state, r' is taken as the sum of Lennard-Jones radii $(\sigma_a + \sigma_b)/2$. There are three such vibrations for the reactant. In the transition state r' is taken as the sum of the Lennard-Jones radius of the side-group atom of the glucose molecule plus the neck radius obtained at the minimum E_0 . The partition function of the reactant state is thus given by a product of vibrational partition functions

$$Q = \prod_{i=1}^f \left[1 - \exp\left(\frac{-h\nu_i}{k_B T}\right) \right]^{-1}. \quad (A.3)$$

The formula for the transition state partition function is the same, except that there are only two vibrations modes ($f=2$) for

penetrant motion in the transition state, since one degree of freedom is taken as the reaction coordinate.

References

- [1] Y. Yampolskii, I. Pinnau, B.D. Freeman (Eds.), *Material Science of Membranes*, John Wiley & Sons, Chichester, 2006.
- [2] A. Schoonman, J. Ubbink, C. Bisperink, M. Le Meste, M. Karel, *Biotechnology* 18 (2002) 139–154.
- [3] J. Krüger, J. Ubbink, *Trends Food Sci. Technol.* 17 (2006) 244.
- [4] D. Kilburn, J. Claude, T. Schweizer, A. Alam, J. Ubbink, *Biomacromolecules* 6 (2005) 864–879.
- [5] Y. Gunning, R. Parker, G. Ring, *Carbohydr. Res.* 329 (2000) 377.
- [6] M. Levine, *Amorphous food and pharmaceutical systems*, Spec. Publ. R. Soc. Chem. (2002) 202.
- [7] S.J. Risch, G.A. Reineccius, *Encapsulation and controlled release of food ingredients*, ACS Symp. Ser. (1995) 590.
- [8] J.P. Amori, A. Huckriede, J. Wilschut, H.W. Frijlink, W.L.J. Hinrichs, *Pharm. Res.* 25 (22) (2008) 1256–1273.
- [9] X.C. Meng, C. Stanton, G.F. Fitzgerald, C. Daly, R.P. Ross, *Food Chem.* 25 (2008) 1406–1416.
- [10] M. le Meste, D. Champion, G. Roudaut, G. Blond, D. Simatos, *J. Food Sci.* 67 (2002) 2444.
- [11] WO2001008504, Foaming ingredient and powders containing it.
- [12] WO2006023564, Non-protein foaming compositions and methods of making the same.
- [13] T. Baks, et al., Schrödinger capsule: a microcapsulate that is open and closed at the same time, *Proc. Phys. Ind.* (2010) 67–84.
- [14] P. Meares, *J. Am. Chem. Soc.* 76 (1954) 3415.
- [15] P. Pandey, R.S. Chauhan, *Prog. Polym. Sci.* 26 (2001) 853.
- [16] S. Townrow, D. Kilburn, A. Alam, J. Ubbink, *J. Phys. Chem. B* 111 (2007) 12643.
- [17] A.A. Gusev, S. Arizzi, U.W. Suter, *J. Chem. Phys.* 99 (1993) 2221.
- [18] A.A. Gray-Weale, R.H. Henchman, R.G. Gilbert, M.L. Greenfield, D.N. Theodorou, *Macromolecules* 30 (1997) 7296.
- [19] R. Kirchheim, *Macromolecules* 25 (1992) 6952.
- [20] W.R. Vieth, J.M. Howell, Hsieh, *J. Membr. Sci.* 1 (1976) 177–220.
- [21] J. Crank, *The Mathematics of Diffusion*, Clarendon Press, Oxford, 1970.
- [22] D. Ehlich, H. Silesco, *Macromolecules* 23 (1990) 1600.
- [23] R. Perry, H. Green, J.O. Maloney, *Perry Chemical Engineers' Handbook*, 7th ed., CRC Press, Boca Raton, 1997.
- [24] K. Ghosal, R.T. Chern, B.D. Freeman, *Macromolecules* 29 (1996) 4360.
- [25] M. Salame, *Poly. Eng. Sci.* 26 (22) (1986) 1543.
- [26] A.Y. Alentiev, Y.M. Yampolskii, *J. Membr. Sci.* 206 (2002) 291–306.
- [27] V.V. Sethuraman, A.J. Hickey, *AAPS Pharm. Sci. Tech.* 3 (28) (2002) 4.
- [28] B.D. Freeman, *Macromolecules* 32 (1999) 375.
- [29] L.M. Robeson, B.D. Freeman, D.R. Paul, B.W. Rowe, *J. Membr. Sci.* 341 (2009) 178–185.
- [30] Y. Yampolskii, V. Shantarovich, *Positron annihilation lifetime spectroscopy and other methods for free volume evaluation in polymers*, pp. 191–210 in Ref. [1] (2006).
- [31] H.J. Takeuchi, *J. Chem. Phys.* 93 (1990) 2062.
- [32] A.A. Gusev, U.W. Suter, *J. Chem. Phys.* 99 (1993) 2228.
- [33] D.N. Theodorou, in: P. Neogy (Ed.), *Diffusion in Polymers*, Marcel Dekker, New York, 1996.
- [34] N. Ramesh, P.K. Davis, J.M. Zielinski, R.P. Danner, J.L. Duda, *J. Polym. Sci. B Polym. Phys.* 49 (2011) 1629.
- [35] M.P. Tonge, R.G. Gilbert, *Polymer* 42 (2001) 501.
- [36] For r_0 , Greenfield and Theodorou's simulation [?] showed that the onset of percolation in the polymer structure occurs for penetrants of radius 1.1 Å. There is an accessible volume cluster for such a penetrant, the so-called infinite cluster, that stretches across the entire simulation cube. They treat polymer and penetrant atoms as having hard sphere radii of $(2^{1/6}\sigma)/2$. In our formulation of the model, we require the percolation radius of a penetrant when the polymer and penetrant molecules are treated as having radii of $\sigma/2$. The difference in radius, Δr , between a molecule of radius $(2^{1/6}\sigma)/2$ and one of radius $\sigma/2$ is $\Delta r = \sigma(2^{1/6}-1)/2$. This suggests that a penetrant of radius $r_0 = 1.1 + \Delta r$ Å can percolate the structure.
- [37] P. Bueche, *J. Chem. Phys.* 21 (1953) 1850.
- [38] D. Seitz, F. Turnbull, in: D. Seitz (Ed.), *Solid State Physics*, Academic New York, 1956.
- [39] N. Muruganandam, W.J. Koros, D.R. Paul, *J. Polym. Sci. Polym. Phys. Ed.* 25 (1987) 1999.
- [40] K. Okamoto, K. Tanaka, O. Yokoshi, H. Kita, *J. Polym. Sci. Polym. Phys. Ed.* 27 (1991) 643.
- [41] T.C. Merkel, V. Bondar, K. Nagai, B.D. Freeman, I. Pinnau, *J. Polym. Sci. B Polym. Phys. Ed.* 38 (2000) 415.
- [42] J.E. Mark (Ed.), *Polymer Data Handbook*, Oxford University Press, Inc., 1999.
- [43] W.J. Koros, G.K. Fleming, S.M. Jordan, T.H. Kim, H. H, *Prog. Polym. Sci.* 13 (1988) 339.
- [44] L.M. Robeson, *Solid State Mater. Sci.* 4 (1999) 549–552.
- [45] L.K. Massey, *Permeability Properties of Plastics and Elastomers: A Guide to Packaging and Barrier Materials*, Plastic Design Library/William Andrew Publishing, Norwich, 2003.
- [46] J. Burke (Ed.), *The Book and Paper Group Annual*, vol. 3, Part 2. The Hildebran Solubility Parameter, The American Institute for Conservation, 1984.
- [47] H.J. Vandenburg, A.A. Clifford, K.D. Bartle, R.E. Carlson, J. Carroll, I.D. Newton, *Analyst* 124 (1999) 1707.
- [48] C.E. Wilkes, J.W. Summers, C.A. Daniels (Eds.), *PVC Handbook*, Hanser Gardner Publications, Inc., 2005.